https://doi.org/10.5194/egusphere-2026-2746
Preprint. Discussion started: 25 June 2026

ENSO Modulation of $PM_{2.5}$ air pollution in Central Kalimantan, Indonesia revealed by a dense network of Purple Air sensors

Ailish M. Graham[1,2], Dominick V. Spracklen[1], James B. McQuaid[1], Richard Rigby[1,3], Hanun Nurrahmawati[4], Devina Ayona[4], Resti Salmayenti[1,5], Kitso Kusin[6], Adi Jaya[6], Thomas E. L. Smith[7], Annisa Alifindira[4], Shofwan Al Banna Choiruzzad[4], Richard Pope[1,2]

1. School of Earth and Environment, University of Leeds, Leeds, UK
2. National Centre for Earth Observation, University of Leeds, Leeds, UK
3. Centre for Environmental Modelling And Computation, University of Leeds, Leeds, UK
4. Faculty of Social and Political Sciences, Universitas Indonesia, Indonesia
5. Department of Geophysics and Meteorology, IPB University, Bogor, Indonesia
6. Centre for International Cooperation in the Sustainable Management of Tropical Peatland, Universitas Palangka Raya, Indonesia
7. London School of Economics and Political Sciences, London, UK

Correspondence to: Ailish M. Graham (a.m.graham@leeds.ac.uk)

Abstract. Peatland fires in Indonesia drive severe air pollution. Studies have focused on El Niño years, therefore neutral and La Niña years remain uncharacterised. We deploy a dense network of $PM_{2.5}$ sensors across Central Kalimantan peatlands between August 2023 and October 2025 to quantify how El Niño–Southern Oscillation (ENSO) modulates the magnitude and spatial variability in dry season $PM_{2.5}$ concentrations. Sensors were installed at urban, rural, and remote locations, spanning El Niño (2023), neutral (2024), and La Niña (2025) dry seasons. During the 2023 El Niño dry season, low rainfall and deep water tables enhanced peatland flammability and supported extensive peat fires. Urban and rural sites exceeded the WHO 24-hour $PM_{2.5}$ guideline on 99 % and 97 % of days. A remote site exceeded these guidelines on 85 % and 24 % of days, with fire smoke influence confirmed by low spatial variability and a dual-peak diurnal cycle across sites, indicating regional pollution rather than local sources. As ENSO conditions shifted to neutral (2024) and La Niña (2025), increased rainfall and shallower water tables reduced fire activity and $PM_{2.5}$ concentrations. In 2024, WHO guideline exceedances fell to 41 % and 12 % at urban and rural sites. Our results indicate that even across non-El Niño years, dry season $PM_{2.5}$ is influenced by regional fire emissions, but the magnitude and spatial variability is modulated by ENSO-phase. Our results demonstrate that dense sensor networks can distinguish regional fire smoke from local pollution, enabling early detection of fire-driven air quality degradation. Reducing peatland fires through restoration and fire management would deliver consistent air quality benefits.

1 Introduction

Across much of Southeast Asia fires are frequently used as cheap and quick tool for land clearance and preparation for agriculture (Page et al., 2002). Fires lead to regional haze episodes that are particularly severe during drought years connected

https://doi.org/10.5194/egusphere-2026-2746
Preprint. Discussion started: 25 June 2026

to El Niño events (e.g. Crippa et al., 2016, Grosvenor et al., 2024, Reddington et al., 2021), with consequences that extend beyond episodic smoke events to sustained regional air quality degradation and major public health burdens.

In Indonesia, forest that was previously cleared for agriculture in Kalimantan and Sumatra is underlain by tropical peat, which has been drained using an extensive network of canals. Canals were used to lower the water table during the establishment of the failed Ex-mega rice project (Ex-MRP), allowing crops to be grown in the peat soil. During particularly dry years (e.g. El Niño years) the water table is further reduced during the dry season (August to November). This means the peat is sufficiently dry for surface fires (Salmayenti et al., 2025), that are used to clear and prepare land, to burn into the carbon rich peat soils beneath. The fires propagate vertically and laterally through the soil subsurface (Mulyasih et al., 2022), via smouldering combustion that dominates emissions of particulate matter (PM) (>95% in 2015 (Wooster et al., 2018)), making peat fires a disproportionately important source of persistent fine particulate pollution.

During dry years, air pollution from Indonesia peatland fires in Kalimantan (62%) and Sumatra (33%) dominate total PM fire emissions in Equatorial Asia (Kiely et al., 2020), leading to dangerous air quality across the region. During 2015, a severe drought year, $PM_{2.5}$ from fires exposed 66.5 million people to $PM_{2.5}$ concentrations above the WHO 24-hour guideline limit (25 mg m^{-3}) for at least half of the dry season (August to October) (Kiely et al., 2020). 51% of the people exposed were from Indonesia but smoke from Sumatra was also transported to Malaysia and Singapore under favourable winds, leading to high population exposure (20 million and 7.98 million, respectively). In total, long-term exposure to peat fire $PM_{2.5}$ in 2015 is estimated to have resulted in 44,041 (95% Confidence Interval: 34,672–53,948) premature deaths (Kiely et al., 2020). These findings underline that Indonesian peat fires are both a local land-management issue and a transboundary air-pollution problem.

Generally, previous studies have focussed on high fire dry seasons, which typically occur in El Niño years such as 2015, 2019 and 2023 (e.g. Kiely et al., 2020; Crippa et al., 2016; Mead et al., 2018), despite fires occurring every dry season. Therefore, little is known about the impact of fires on air quality in the region in non-El Niño (neutral and La Niña) years with fewer fires. Although the overall health impact is likely to be smaller, populations close to where fires occur are still likely to be exposed to high $PM_{2.5}$ concentrations.

Previous modelling studies focussed on estimating the impacts of Indonesian fires on air quality have relied on the limited number of monitoring sites where air pollution is routinely monitored. These monitoring sites are often far from fires or only provide weekly-mean air pollutant concentrations (e.g. Crippa et al., 2016; Kiely et al., 2019, 2020). Therefore, limiting the evaluation of modelling studies and fire emissions inventories. However, more recent work has utilised networks of low-cost $PM_{2.5}$ sensors, located close to fires during El Niño dry seasons (Grosvenor et al., 2024; Graham et al., 2024). Both studies deployed Purple Air sensors in Palangka Raya, the capital city of Central Kalimantan. Measurements from the low-cost sensors indicated that daily-mean $PM_{2.5}$ concentrations in the city exceeded 500 µg m^{-3} in 2019 and 400 µg m^{-3} in 2023. In addition, in

https://doi.org/10.5194/egusphere-2026-2746
Preprint. Discussion started: 25 June 2026

2023, sensors were deployed in the wider Pulang Pisau region of Central Kalimantan (to the south of Palangka Raya), where fires frequently occur. Measurements indicated that daily-mean $PM_{2.5}$ concentrations widely reached 400-500 µg m^{-3} in rural areas that were in closer proximity to fires. While these studies revealed the severity of pollution during El Niño fire years, they did not resolve how pollution patterns evolve across contrasting ENSO phases.

Recent studies in other regions have leveraged dense networks of low-cost $PM_{2.5}$ sensors to assess the relative contributions of local versus regional emission sources to observed $PM_{2.5}$ concentrations (Frederickson et al., 2022). The substantially increased site density and high temporal resolution afforded by low-cost sensor deployments enables more detailed characterisation of both spatial and temporal variability in air pollution levels than is possible with reference grade monitoring networks. These capabilities stem from the comparatively low cost, compact size, and simple deployment requirements of such sensors, which typically need only a power supply and Wi-Fi connection.

In this work, we analyse long-term $PM_{2.5}$ monitoring data from a network of low-cost $PM_{2.5}$ sensors deployed across Central Kalimantan peatlands. Ambient outdoor $PM_{2.5}$ concentrations were monitored between August 2023 and October 2025, spanning an El Nino dry season (2023), a neutral dry season (2024) and a La Nina dry season (2025), as well as two wet seasons. This allowed us to explore the impact of ENSO-phase on dry season $PM_{2.5}$ concentrations across Central Kalimantan peatlands in detail for the first time, using ground-based monitoring. Beyond quantifying ENSO controls on pollution magnitude, this framework also enables assessment of how spatial variability in $PM_{2.5}$ can be used to distinguish regional fire influence from local emissions. By spanning contrasting hydroclimatic conditions, this study provides a more complete understanding of peat-fire air quality impacts across climate states, rather than during extreme El Niño conditions alone.

2 Methods

2.1 Sensor Network

2.1.1 Location of Sensors

We maintained a network of between 13 and up to 110 low-cost $PM_{2.5}$ sensors at indoor and outdoor locations across Pulang Pisau, Central Kalimantan, Indonesia between August 2023 and October 2025. The network included between 4 and 42 outdoor sensors (2023-2025) which we focus on in this paper (Figure 1). Since the number of sensors varied over the study period, we give details of the sensor network that was deployed for each dry season (2023-2025) in the following sections and include an overview of the sensor network in Figure 1.

Sensor Network 2023

The network included 4 outdoor long-term monitors that have been deployed since August 2023 (Supplementary Material: Table S1 and Figure S1). These sensors were deployed in August 2023 as part of a small network of 13 indoor and outdoor Purple Air PA-II sensors across urban, rural and remote locations in Pulang Pisau, Central Kalimantan, Indonesia (Graham et

https://doi.org/10.5194/egusphere-2026-2746
Preprint. Discussion started: 25 June 2026

al., 2024). The sensors were initially deployed to measure $PM_{2.5}$ concentrations during an El Niño dry season. 4 of the outdoor sensors have remained in the same location since 2023 to provide long-term monitoring across the region (Table S1). All long-term monitoring sensors remained in the same location from August 16th 2023 to January 8th 2025, except the sensor at the remote site (Sebangau), which stopped working and was replaced on October 8th 2024.

Sensor Network 2024

In June 2024 we deployed a further 42 outdoor sensors across the same region. The sensors were deployed from July 1st 2024 to January 8th 2025 across 3 rural locations (Tanjung Taruna, Tumbang Tahai and Gohong) and 2 urban locations (Kereng and Palangka Raya) (Figure 1). We deployed sensors at households, offices, schools and hospitals across all locations (except Gohong which had no household sensors). In addition, sensors were deployed across a range of other locations in Palangka Raya, including hotels, restaurants, university buildings and religious buildings. However, for simplicity, we have only included outdoor sensors at households, hospitals, offices, educational buildings and a remote location. The details of outdoor sensors used in this study can be found in Supplementary Material: Table S2 (including a collocation site) and Figure S2. Our full sensor network included the deployment of 103 indoor and outdoor sensors. Across Palangka Raya we deployed 54 indoor and outdoor sensors, providing one of the densest sensor networks anywhere in the world (1 sensor per 2.8 km^2) (Table 2).

Sensor Network 2025

A smaller network of sensors is still deployed in Palangka Raya to date and is managed by the Centre for International Cooperation in Sustainable Management of Tropical Peatland (CIMTROP) at the University of Palangka Raya. We utilise several of the outdoor sensors (6 in total) from this remaining network to extend the analysis to the 2025, including the majority of the dry season (August 1st to October 12th 2025). We give details of the outdoor sensors in the Supplementary Material: Table S3 and Figure S3.

Although at most locations a pair of sensors was deployed, with 1 indoor and 1 outdoor sensor, in this study we focus on ambient outdoor air pollution. The outdoor sensors were mounted in a sheltered location ~1–2 m from the ground, away from where people smoke.

https://doi.org/10.5194/egusphere-2026-2746
Preprint. Discussion started: 25 June 2026

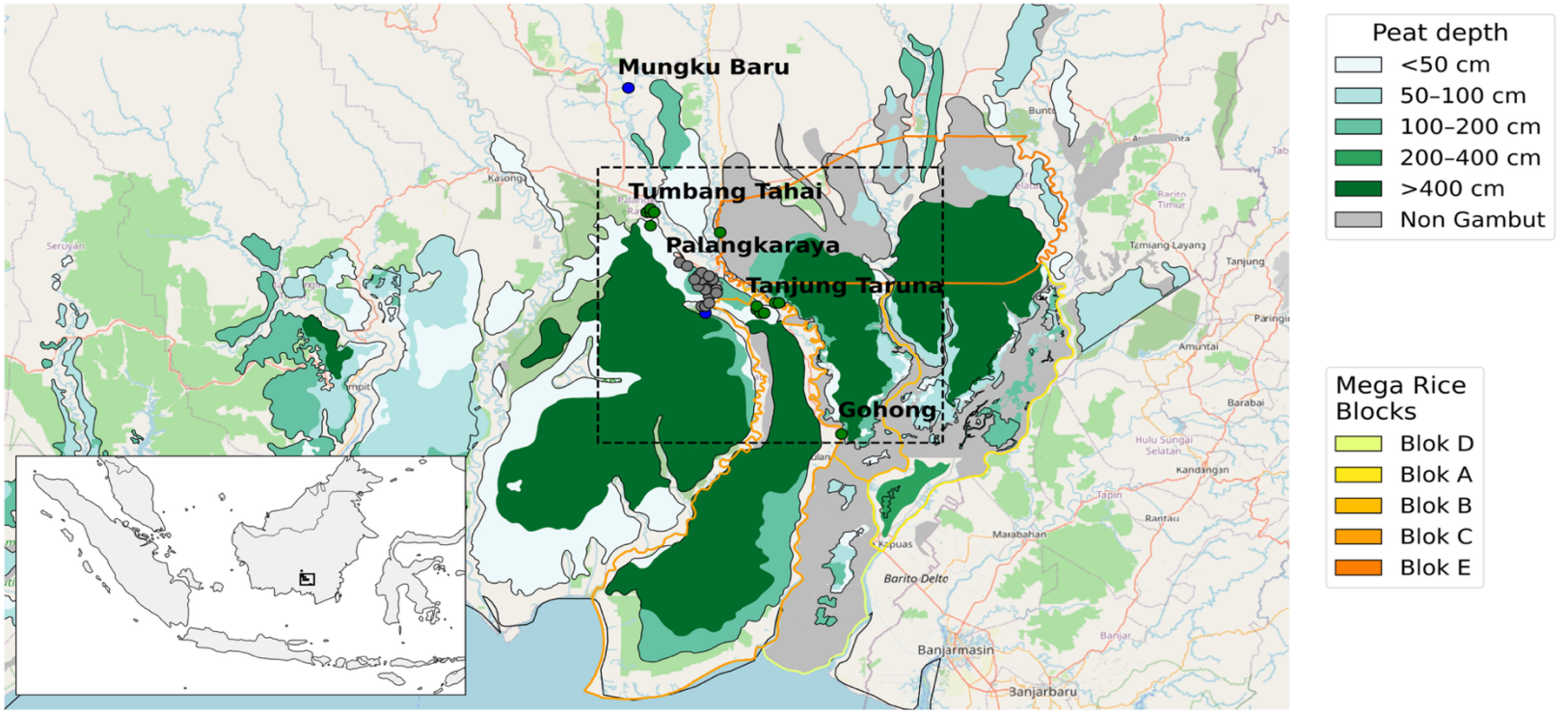

Figure 1. Map of study domain (inset: within Indonesia) in Pulang Pisau, Central Kalimantan. Locations of outdoor Purple Air sensor locations deployed across the study domain between 2023 and 2025 are indicated by coloured circles. Sensors are coloured by site type (urban: grey, rural: green and remote: blue). Latitude and longitude of locations have been limited to two decimal places to maintain volunteer anonymity. The names of key sensor deployment sites are included for reference. The location and depth of underlaying peatlands and their depth are also shown, alongside the boundaries for the Ex-Mega rice blocks. For more information on sensor locations each dry season (2023-2025) refer to Supplementary Material Table S1-3 and Figure S1-3.

https://doi.org/10.5194/egusphere-2026-2746
Preprint. Discussion started: 25 June 2026

2.1.2 Sensor Information

PA-II sensors report $PM_{2.5}$ concentrations at 2-min time resolution. Inside the PA-II sensor two Plantower PMS5003 laser particle counters (labelled channel A and channel B) calculate the size of particles. Air is drawn into each sensor past a laser at a flow rate of 0.1 L min^{-1}. Particle size is calculated using Mie theory and a photodiode detector that converts scattered light into a voltage pulse. Particle counts are split into 6 size bins (0.3, 0.5, 1, 2.5, 5 and 10 µm) before an algorithm provided by Purple Air is used to convert particle counts into mass concentrations for PM_1, $PM_{2.5}$ and PM_{10} (all in µg m^{-3}). The mass concentration range of the sensors is 0–500 µg m^{-3} with a mass concentration accuracy of ±10 µg m^{-3} between 0 and 100 µg m^{-3} and ±10% between 100 and 500 µg m^{-3}. The sensors operate effectively in a temperature range of −10 °C to 60 °C and 0% to 99% relative humidity.

Low-cost sensors, such as Plantower PMS5003 used in Purple Air sensors (PA-II), do not always agree well with reference grade measurements that are made using different principles (e.g. beta attenuation monitoring (BAM) instruments). There are several reasons for the disagreement. Firstly, BAM instruments report mass concentrations under specific temperature and relative humidity conditions (EPA, 2016). Whereas low-cost sensors measure in ambient conditions where relative humidity is not controlled. As humidity increases particles grow hygroscopically leading to increased particle size, and thus an overprediction in particle mass in low-cost sensor sensors. Thus, accounting for hygroscopic growth at high relative humidities is needed when using low-cost sensors. Accuracy assessments of the Plantower PMS5003 particle counters have found them to perform well against regulation certified air quality monitoring equipment, once corrected for variability in relative humidity (Chan et al., 2021). Secondly, low-cost sensors can generally only measure particles >0.3 µm in size and so will underreport $PM_{2.5}$. To address this, underreporting of small particles is corrected for during factory calibration. The Plantower PMS5003 sensors are calibrated in-factory using ambient aerosol from several Chinese cities (Malings et al., 2020). Finally, differences in aerosol composition and size distribution between ambient deployment and factory calibration can cause further errors.

2.1.3. Quality control

We follow the quality control procedures of Mattheiu-Campbell *et al.,* (2024) and Barkjohn *et al.,* (2021) and perform quality control procedures on $PM_{2.5}$ concentrations from the cf_1 channel. Firstly, we use a lower and upper detection limit of ≥1.5 µg m^{-3} and ≤1000 µg m^{-3}, respectively, and remove any values which lie outside of these limits (Mattheiu-Campbell et al., 2024). Next, we consider agreement between the 2 sensors (channels A and B), we consider low (≤25 µg m^{-3}) and high (>25 µg m^{-3}) concentrations separately. In the case of low concentrations, we remove observations where channels A and B differ by more than 5 µg m^{-3}. For high concentrations we remove observations where channels A and B differ by more than 50%. Following this, channels A and B are averaged, and both hourly and daily means are calculated. An hourly mean is calculated if >90% of data is available (27/30 2-minute values are available). For 2023 and 2024 data, we calculate the daily mean if >75% of data is available (18/24 hours are available). For 2025, we relax this threshold to 50% since we are reliant on data reported via a Wi-Fi upload rather than from the internal SD card. This meant that data availability for 2025 was lower due to

https://doi.org/10.5194/egusphere-2026-2746
Preprint. Discussion started: 25 June 2026

interruptions to the Wi-Fi signal. Daily mean data from 2024 was used during calibration of the Purple Air sensors to a reference grade site in Palangka Raya.

2.1.4. Relative Humidity Adjustment

We collocated 3 Purple Air sensors with a reference grade air quality monitor at the Indonesian Ministry of Environment and Forestry (KLHK) in Palangka Raya for the period July 1st 2024 to January 8th 2025. This allowed us to produce a region-specific relative humidity (RH) adjustment for the sensors using multiple linear regression (MLR) (McFarlane et al., 2021, Mattheiu-Campbell et al., 2024, Barkjohn et al., 2021). More details of our region-specific RH adjustment are given in the Supplementary Material (Supplementary Material 2 and Figure S4). In brief, the region-specific RH adjustment regressor score was 0.69. We found that including an additive RH term improved Purple Air performance substantially (r= 0.89, NMBF=0.02, NMAE=0.17, RMSE=10.5) (Figure S2). Therefore, the RH adjustment was applied to hourly and daily data from all Purple Air sensors across the full dataset (2023-2025).

2.1.5 Purple Air $PM_{2.5}$ Concentrations

To explore the influence of local and regional pollution sources during different seasons from August 2023 to January 2025 we use $PM_{2.5}$ concentrations from outdoor sensors. For each site we calculate the daily-mean and the 14-day rolling mean $PM_{2.5}$ concentrations as well as the coefficient of variation (CoV) across the network. CoV is an indicator the heterogeneity of $PM_{2.5}$ across sites. High CoV indicates large differences between sites, consistent with the influence of local emission sources that generate strong, short scale spatial gradients in $PM_{2.5}$ concentrations. In contrast, low CoV reflects spatially uniform $PM_{2.5}$ concentrations, characteristic of periods dominated by regional pollution transported over larger spatial scales under large-scale meteorological conditions. We use CoV alongside $PM_{2.5}$ concentrations to jointly identify periods when local sources or regional transport exert the dominant influence on observed $PM_{2.5}$ concentrations.

2.2 El Niño Southern Oscillation Index

To explore the relationship between El Niño Southern Oscillation Index (ENSO), $PM_{2.5}$ concentrations and other key parameters (fire counts, water table depth) we use the Oceanic Niño Index (ONI) from the NOAA Climate Prediction Centre (CPC) (NOAA, 2026). The ONI uses a 3-month running mean of sea surface temperature anomalies in the Niño 3.4 region to determine ENSO phase. El Niño conditions are characterised by an ONI ≥+0.5 °C, while La Niña conditions are characterised by an ONI ≤-0.5 °C. Neutral conditions lie between these (≥-0.5 °C and ≤+0.5 °C). An El Niño or La Niña event must persist for at least five consecutive overlapping 3-month periods to be categorised.

2.3 Pulang Pisau Peatland Fire Count and $PM_{2.5}$ Fire Emissions

We use fire hotspot detections from the Visible Infrared Imaging Radiometer Suite (VIIRS) sensor aboard Suomi-National Polar-orbiting Partnership (S-NPP) satellite (Schroeder et al., 2014). VIIRS has been in orbit since 2011 and has an overpass

https://doi.org/10.5194/egusphere-2026-2746
Preprint. Discussion started: 25 June 2026

time of 13:30. VIIRS detects active fires at 375 m spatial resolution. We subsample fire hotspot detections using a shapefile for Pulang Pisau peatlands (see Figure 1 for extent) to isolate fires that occurred on peat.

We use $PM_{2.5}$ fire emissions from Global Fire Assimilation System (GFAS) (Kaiser et al., 2012). GFAS produces daily estimates of biomass burning emissions at 0.1° resolution. Emissions are estimated using satellite-based Fire Radiative Power (FRP) approach. FRP is used to estimate emissions in two steps. First, FRP is converted to dry matter consumed. Then biome specific emissions factors, from field and laboratory studies, are applied to dry matter consumed to estimate emissions of key air pollutant species. In this study we take gridded daily $PM_{2.5}$ emissions and subsample them over Pulang Pisau peatlands. We choose to use GFAS fire emissions over other fire emissions datasets for two main reasons. GFAS includes below-ground burning from peat fires and it is available at near-real time.

We sum fire counts and $PM_{2.5}$ fire emissions. This allows us to examine the change in total fire counts and fire emissions occurring on Pulang Pisau peatlands between August 1st 2023 and October 12th 2025.

2.4 Pulang Pisau Peatland Water Table Depth

We use peat water table depth (WTD) from NASA's Level 4 Soil Moisture Active Passive Product (SMAP) to examine dry season WTD in Pulang Pisau peatlands between 2023 and 2025. SMAP WTD has a spatial resolution of 9 km and temporal resolution of 3 hours. The Level 4 data assimilates SMAP measurements of soil moisture into NASA Goddard Earth Observing System, Version 5 (GEOS-5) land data assimilation system (LDAS) to simulate the vertical transfer of soil moisture between the surface and root zone reservoirs (Reichle at al., 2018). The land-surface model is driven with meteorological reanalysis and includes soil moisture transfer between the surface and root zones (up to 1 m depth). The SMAP WTD is both spatially and temporally complete. We calculate the average Pulang Pisau peatland WTD between August 1st and October 31st for 2023, 2024 and 2025. This allows us to investigate the variability in WTD between 2023-2025 dry seasons.

2.5 Pulang Pisau Peatland Precipitation

To examine changes in precipitation between the 2023-2025 dry seasons, we use monthly mean precipitation from the European Centre for Medium Range Weather Forecasting (ECMWF) 5th generation reanalysis dataset (ERA5) at 0.25 degree spatial resolution. We subsample the dataset over Pulang Pisau peatlands and calculate the grid-cell average monthly total precipitation.

3. Results

Our study covers August 2023–October 2025, spanning all three ENSO phases (El Niño, Neutral and La Niña) (Figure 2).

https://doi.org/10.5194/egusphere-2026-2746
Preprint. Discussion started: 25 June 2026

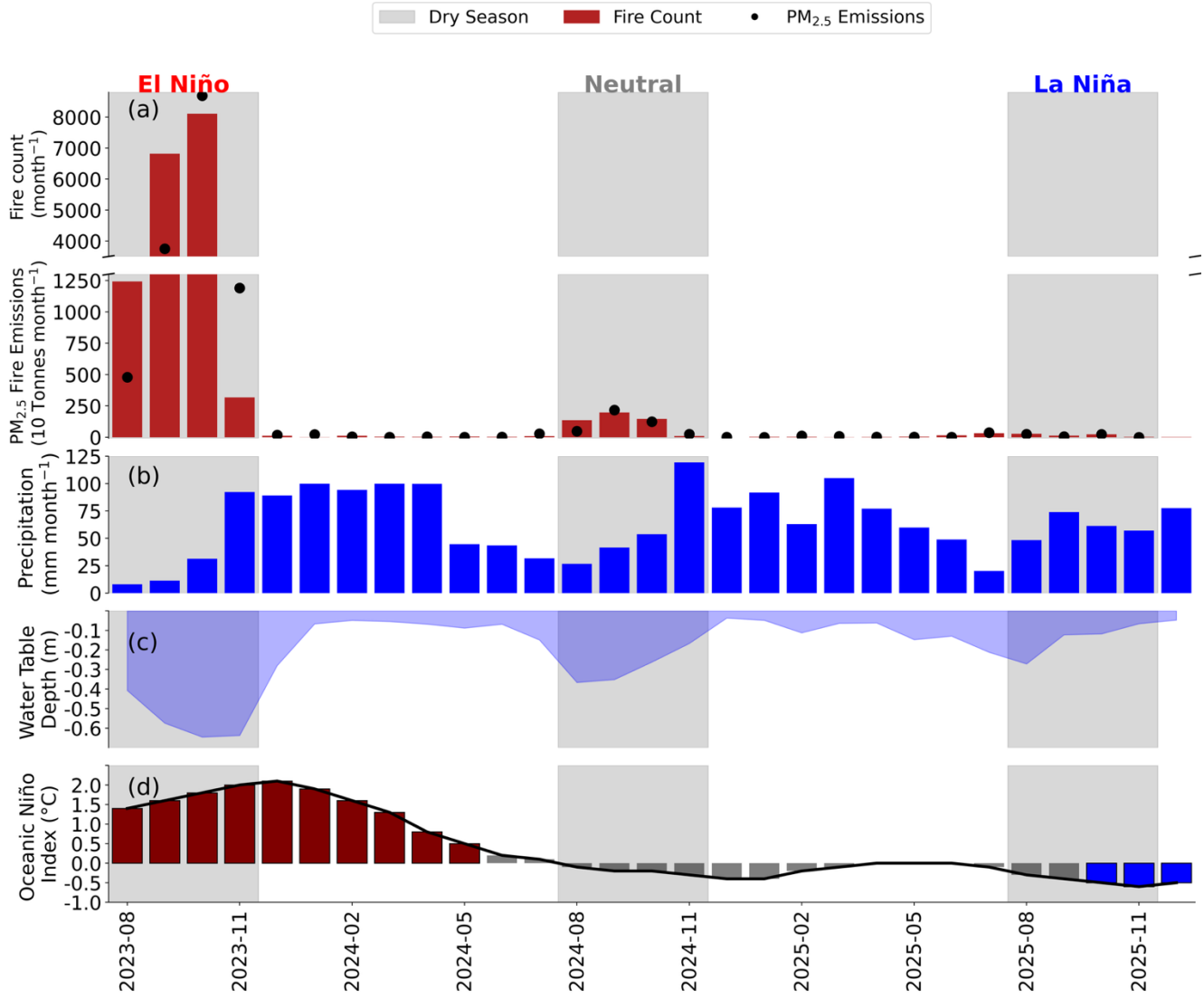

Figure 2. Timeseries of (a) monthly summed Pulang Pisau peatland fire counts (red bars) and Pulang Pisau peatland $PM_{2.5}$ fire emissions (black scatter) (10 Tonnes month^{-1}) (b) Water table depth below the surface (m) [blue shading] and (c) monthly total, grid-cell average Pulang Pisau peatland precipitation (mm month^{-1}) and (d) El Niño Southern Oscillation phase (°C) (coloured bars) between August 2023 and December 2025. The dry season (August to November) each year (grey shading) and the El Niño Southern Oscillation phase are indicated above grey shading in (a).

From August to November 2023, moderate to strong El Niño conditions (1.4–2.0 °C) (Figure 2 (d)) suppressed rainfall and raised temperatures across Indonesia, producing severe drought. Pulang Pisau peatlands experienced very low rainfall (8–31 mm month^{-1}) (Figure 2 (b)) and deep water tables (–0.41 to –0.65 m) (Figure 2 (c)), amplified by extensive drainage. The

https://doi.org/10.5194/egusphere-2026-2746
Preprint. Discussion started: 25 June 2026

resulting high peat flammability enabled fires, which are commonly used for land clearing, to spread easily above and below ground, yielding high monthly fire counts (1,242–8,109 month^{-1}) and $PM_{2.5}$ emissions (4.79–86.9 Gg $PM_{2.5}$ month^{-1}) (Figure 2 (a)). These conditions indicate that ENSO influences regional air pollution through hydroclimatic control on peat flammability, rather than through fire occurrence alone. The coincidence of deep water tables and sharply elevated emissions also suggests a threshold like response, whereby substantial increases in fire activity occur once peat drying exceeds critical limits.

Rainfall increased substantially in December 2023 (89 mm month^{-1}), raising the water table (–0.28 m) and reducing fire activity and associated emissions (12 fires, 0.17 Gg $PM_{2.5}$ month^{-1}). Rainfall (41–119 mm month^{-1}) and shallow water tables (–0.28 to –0.05 m) persisted through the wet season, keeping fire counts (1–12) and emissions (0.007–0.27 Gg month^{-1}) low. ENSO conditions weakened throughout early 2024, shifting from strong El Niño (≥2 °C) to neutral by June 2024 (≤0.5 °C).

The 2024 dry season occurred under neutral ENSO conditions (–0.1 to –0.3 °C). Rainfall was substantially higher (27–119 mm month^{-1}) than during the 2023 dry season, and water tables remained closer to the surface (–0.16 to –0.37 m). Consequently, fire counts (10–197) and $PM_{2.5}$ emissions (0.23–2.17 Gg $PM_{2.5}$ month^{-1}) are one to two orders of magnitude lower than in 2023. This contrast implies substantial hydroclimatic suppression of peat fire emissions under neutral conditions, and suggests that lower fire years are not simply weaker versions of El Niño years, but may reflect different pollution regimes.

Rainfall increased again in December and stayed high until April 2025 (63–105 mm month^{-1}), then declined toward the next dry season (April–July: 49–77 mm month^{-1}). Water tables followed the same pattern, remaining shallow until April (–0.04 to –0.06 m) before deepening slightly (–0.12 to –0.15 m). Fire activity remained minimal (0–4 fires; 0–0.17 Gg $PM_{2.5}$ month^{-1}) until June, indicating a lag between declining rainfall, water table drawdown, and fire occurrence. ENSO remained neutral throughout.

At the onset of the 2025 dry season, the ONI declined and crossed the La Niña threshold in October (≤–0.5 °C). Rainfall remained higher than in the 2023 and 2024 dry seasons (48–74 mm month^{-1}). Water tables were deepest in August (–0.27 m) but rose steadily to November (–0.07 m), limiting fire spread. The dry season fire counts (3–27) and $PM_{2.5}$ emissions (0–0.024 Gg $PM_{2.5}$ month^{-1}) were far lower than in the corresponding periods of 2023 and 2024. Together, the progressive transition from El Niño to Neutral and La Niña conditions reveals a strong ENSO modulation of peat fire emissions that is mediated by hydrological controls on fuel availability and combustibility. Across all three years, progressively wetter hydroclimatic conditions were associated with reduced water table drawdown, lower fire emissions, and weaker regional pollution forcing, highlighting a coherent climate–hydrology–fire–air quality linkage.

https://doi.org/10.5194/egusphere-2026-2746
Preprint. Discussion started: 25 June 2026

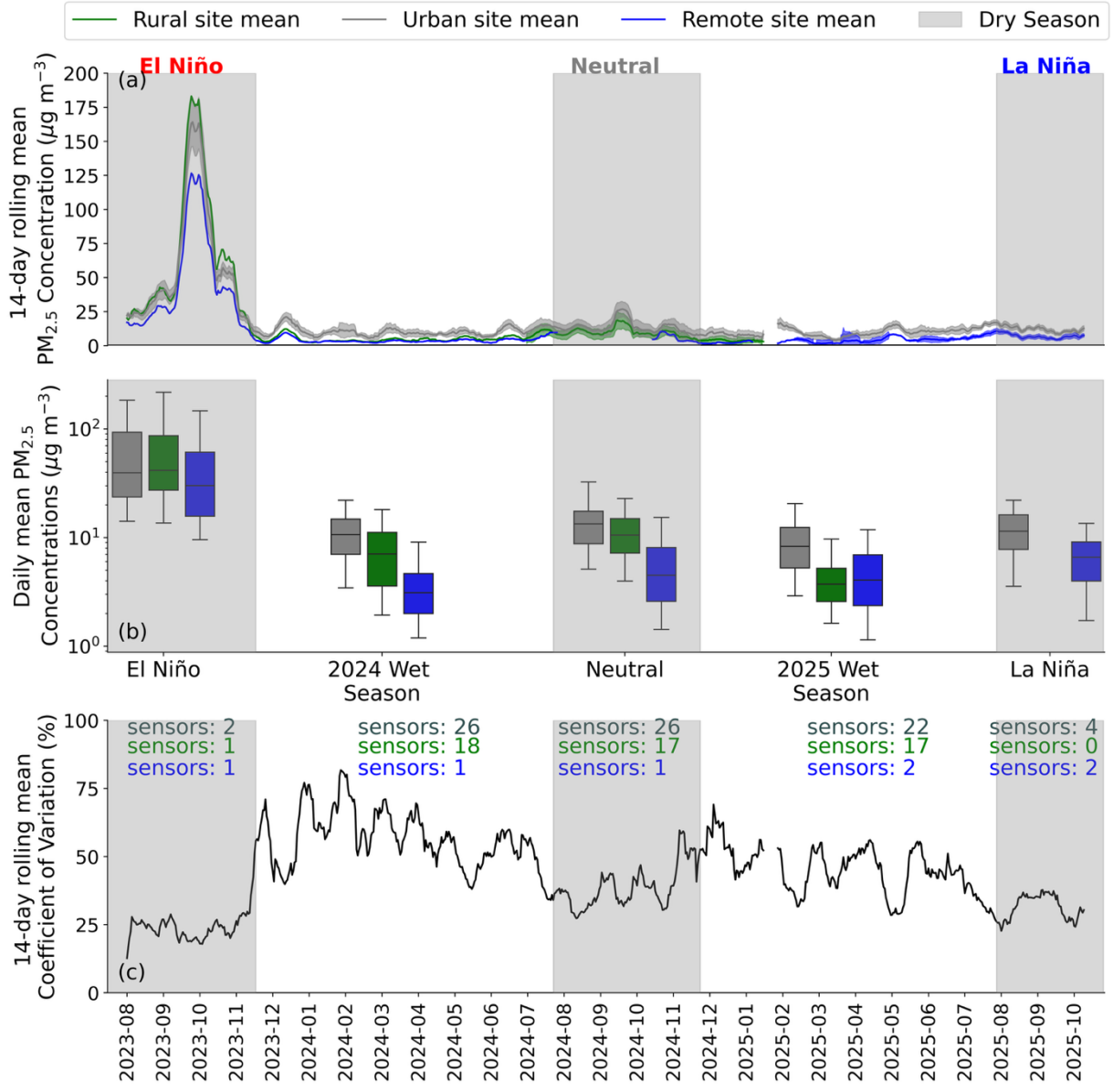

Figure 3. Timeseries of (a) Purple Air 14-day rolling-mean daily mean $PM_{2.5}$ concentrations across urban (grey), rural (green), remote (blue) sites (b) daily mean $PM_{2.5}$ concentrations across urban (grey), rural (green), remote (blue) sites and (c) 14-day rolling-mean coefficient of variation for $PM_{2.5}$ across all sites between August 2023 and October 2025. The dry season (August to November) each year (grey shading) and the El Niño Southern Oscillation phase are indicated in (a).

https://doi.org/10.5194/egusphere-2026-2746
Preprint. Discussion started: 25 June 2026

During the 2023 dry season (August-October) the Oceanic Niño Index (ONI) was 1.6 °C, indicating strong El Niño conditions. During this time, across Pulang Pisau peatlands there was high fire activity (16,169 fires) and the water table was low (-0.55 m) (Figure 2). The concurrence of deep water tables, high fire counts and widespread exceedances suggests a tightly coupled hydroclimate–fire–exposure response under El Niño conditions. The mean dry season $PM_{2.5}$ concentration was similar (78.4 and 74.0 μg m^{-3}) at the rural and urban site, while at a remote site it was substantially lower (54.2 μg m^{-3}). Through the dry season the remote, rural and urban site exceeded the WHO 24-hour $PM_{2.5}$ guideline limit on 64, 74 and 75 days (84, 97 and 99% of dry season days) and the Indonesian 24-hour $PM_{2.5}$ guideline limit on 21, 31 and 27 days (28, 31 and 36% of dry season days). Despite lower $PM_{2.5}$ concentrations at the remote site, the very high frequency of WHO exceedances (84%) indicates regional smoke exposure extended well beyond areas proximate to active fires. That exceedances of the WHO guideline occurred on nearly every dry season day at populated sites highlights the chronic rather than episodic exposure conditions during severe fire years. In contrast, in the 2024 dry season the ONI was -0.2 °C, indicating neutral ENSO conditions. During 2024, Pulang Pisau peatland fire activity was an order of magnitude lower than 2023 (479 fires) and the water table was also much closer to the surface (-0.33 m). The dry season mean $PM_{2.5}$ concentrations were substantially lower than 2023 at the remote (10.2 μg m^{-3}), rural (10.1 μg m^{-3}) and urban site (16.8 μg m^{-3}). The sharp reduction in exceedances relative to 2023 suggests a highly nonlinear sensitivity of pollution exposure to changes in peatland drying and fire activity. The number of exceedances of the WHO 24-hour $PM_{2.5}$ guideline limit and Indonesian 24-hour $PM_{2.5}$ guideline limit reduced considerably at the remote (WHO: 3 days (3%) and Indonesia: 0 days (0%)), rural (WHO: 11 days (12%) and Indonesia: 0 days (0%)), and urban site (WHO: 38 days (41%) and Indonesia: 1 days (1%)). The 2025 dry season was characterised by weak La Niña conditions (ONI: -0.5 °C). As a result, fire activity was two orders of magnitude lower than 2023 (63 fires) and the water table was also much shallower (-0.17 m). The progressive reduction in fire activity from El Niño to Neutral to La Niña provides evidence of strong ENSO modulation not only of emissions, but of probability of population exposure to exceedances in air quality limits. Dry season mean $PM_{2.5}$ concentrations in 2025 were the lowest of all three years at both the remote (6.6 μg m^{-3}) and urban site (11.7 μg m^{-3}). During 2025, no days at either site exceeded the Indonesian 24-hour $PM_{2.5}$ guideline limit and few days exceeded the WHO guideline limit at the urban site (15 days (21%)) or the remote site (1 day (1%)). This indicates that dry season exceedances of the 24-hour $PM_{2.5}$ guideline limits are driven by fire activity and peatland flammability, which are controlled by ENSO-phase. More broadly, these results suggest that ENSO-phase modulates not only mean $PM_{2.5}$ concentrations, but also the frequency, persistence and spatial extent of hazardous pollution exposure. The strong correspondence between ONI, water-table depth, fire activity and exceedance frequency also points toward the potential for hydroclimatic indicators to support predictive early-warning systems for smoke exposure risk. Viewed across all years, exceedance behaviour exhibits a threshold-like response, with strong increases in exposure occurring under sufficiently dry peat conditions, reinforcing the central role of peat hydrology in regulating air quality impacts.

https://doi.org/10.5194/egusphere-2026-2746
Preprint. Discussion started: 25 June 2026

3.3 Diurnal Cycle of $PM_{2.5}$ Concentrations

To examine seasonal differences in the diurnal cycle of $PM_{2.5}$ concentrations we divided the full times series into four periods: the 2023 El Niño dry season, the 2024 neutral dry season, the 2025 La Niña dry season and the two wet seasons (2023–2024 and 2024-2025, which were combined). Examining diurnal structure provides additional insight into source influences that cannot be inferred from daily mean concentrations alone, particularly in distinguishing regional smoke contributions from locally driven emission signatures.

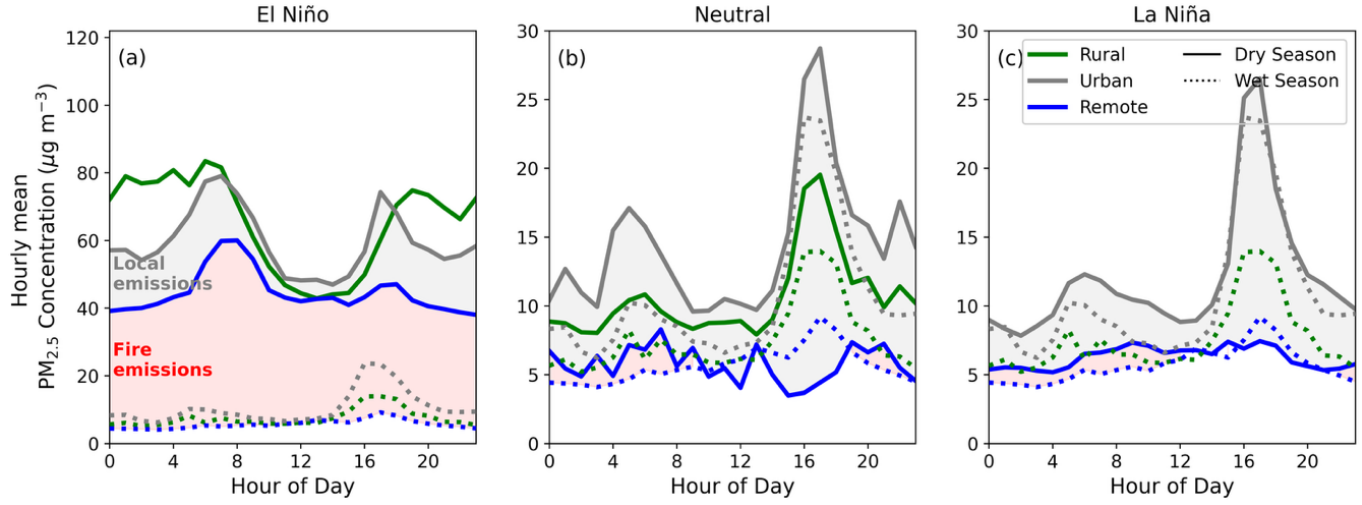

Figure 4. Diurnal cycle of hourly mean $PM_{2.5}$ concentrations in urban (grey), rural (green) and remote (blues) sites for (a) an El Niño dry season (August 16th to November 30th 2023) (b) a neutral dry season (August 1st 2024 to November 30th 2024) and (c) a La Nina dry season (August 1st to October 12th 2025). In each panel the mean diurnal cycle across the 2023/34 and 2024/25 wet seasons (December 1st to July 31st) is also shown (dashed line) and. Key source contributions to $PM_{2.5}$ concentrations during different periods are annotated. The difference between remote site wet season (blue dashed) and dry season (blue solid) $PM_{2.5}$ concentrations indicates the influence of fire emissions. The difference between remote site dry season (blue solid) and urban site dry season (grey solid) $PM_{2.5}$ concentrations indicates the influence of local emissions.

During the 2023 El Niño dry season, urban and rural sites show a dual-peak diurnal cycle, with a strong morning peak (06:00–09:00; >61–83.5 μg m^{-3}) and a secondary evening peak (16:00–20:00; ~49.9–74.8 μg m^{-3}) (Figure 4 (a)). The persistence of a common dual-peak structure across sites suggests regional smoke loading provides an elevated background upon which local emissions are superimposed. The remote site exhibited lower concentrations (39.2-60.1 μg m^{-3}) and a weaker evening peak, suggestive of limited local emissions (e.g. traffic, rubbish burning) compared with the urban and rural sites (grey shading). This contrast between remote and populated sites provides independent evidence that local anthropogenic emissions contribute primarily to the secondary evening enhancement, while much of the daytime baseline reflects regional fire influence. Elevated

https://doi.org/10.5194/egusphere-2026-2746
Preprint. Discussion started: 25 June 2026

overnight $PM_{2.5}$ concentrations at all sites indicate pollutant trapping as the boundary layer collapses. This also suggests boundary layer dynamics may amplify fire related $PM_{2.5}$ exposure during nighttime and early morning hours. The contrast between wet and dry season behaviour at the remote site also provides an estimate of fire contributions (red shading). During the wet season, concentrations at the remote site remained 4.1-9.2 μg m^{-3} throughout the day, with no clear diurnal cycle, implying that fires add 33.6-54.8 μg m^{-3} to dry season $PM_{2.5}$ (red shading). The absence of pronounced diurnal structure at the remote site during the wet season, compared with strong dry season enhancement, further supports the dominance of regionally transported smoke during El Niño conditions.

During the neutral 2024 dry season and La Niña 2025 dry season, the diurnal cycle of $PM_{2.5}$ concentrations was similar, with only small dry season increases (~3.5-5 μg m^{-3}), compared with the wet seasons. The marked weakening of the dry season diurnal enhancement relative to 2023 indicates substantial suppression of the regionally coherent fire influence under non-El Niño conditions. Urban (and in 2024 rural) sites exhibited a clear evening peak (17:00–19:00) in $PM_{2.5}$ concentrations, reaching 13.9–23.5 μg m^{-3} in the wet season and 19.5–28.7 μg m^{-3} in the dry seasons, with minimal morning enhancement compared with 2023. The persistence of evening peaks despite reduced fire activity suggests local emissions become relatively more important when regional smoke forcing is reduced. The remote sites have no clear diurnal cycle in either season in 2024 and 2025. However, $PM_{2.5}$ concentrations are generally higher (up to 3.3 μg m^{-3}) in the dry seasons, indicative of a small fire influence. These modest but coherent dry season enhancements imply that regional smoke influence persists even during neutral and La Niña years, albeit at substantially reduced intensity. Taken together, the shift from a dual-peak, regionally elevated diurnal cycle in 2023 to weaker, locally dominated diurnal cycles in 2024–2025 reveals a transition in source regime structure, which is strongly modulated by ENSO-phase. This suggests ENSO-phase affects not only the magnitude of $PM_{2.5}$ pollution, but also the temporal signature of source contributions, a feature that is impossible to capture using daily-mean concentrations alone. More broadly, these results show that diurnal behaviour provides an additional line of evidence for distinguishing regional fire emissions from local sources within dense sensor networks.

4. Discussion

4.1 ENSO controls on hydrology, fire activity and $PM_{2.5}$ concentrations

We deployed a network of low-cost $PM_{2.5}$ sensors across Pulang Pisau (Central Kalimantan) peatlands between August 2023 and October 2025. This network, ranging from 4 to 46 outdoor sensors, measured $PM_{2.5}$ concentrations across three dry seasons, including an El Niño (2023), neutral (2024), and La Niña (2025) dry season, and two wet seasons. This multi-year dataset captures a rare natural experiment across contrasting hydroclimatic states, enabling assessment of how climate variability propagates from peat hydrology through to fire emissions and air quality impacts.

Our results indicate that ENSO phase strongly influences water table depth, fire activity and dry season $PM_{2.5}$ concentrations across Pulang Pisau. More broadly, the results indicate that ENSO acts as a first-order control on regional smoke exposure

https://doi.org/10.5194/egusphere-2026-2746
Preprint. Discussion started: 25 June 2026

through modulation of peatland flammability. During the 2023 El Niño dry season, suppressed rainfall (8-31 mm month^{-1}) and deep peatland water tables (< -27 to -54 cm) enabled extensive peat fires, driving increased $PM_{2.5}$ concentrations. The close correspondence between deep water tables and extreme smoke exposure suggests a threshold-like response in which relatively modest hydrological shifts can trigger disproportionate increases in fire emissions. During the 2023 dry season, Pulang Pisau peatlands experienced over 16,169 fires and fire $PM_{2.5}$ emissions exceeded 4.5-86.9 Gg month^{-1}.

In 2024, increased precipitation (27-54 mm month^{-1}) raised water table depths (-37 to -26 cm), reducing fire activity by a factor of 250 and fire emissions by a factor of 33. A comparison of dry and wet season concentrations suggests fire increased $PM_{2.5}$ concentrations of <0.1 µg m^{-3} (0 to 3.3 µg m^{-3}). Scaling the fire-enhanced $PM_{2.5}$ estimate of 38.9 µg m^{-3} (33.6-54.8 µg m^{-3}) in 2023 by the difference in fire emissions, would suggest a fire enhancement in 2024 of ~1.2 µg m^{-3}. The disparity in totals could be due to increased wet deposition during the 2024 dry season as mean monthly precipitation was substantially higher across Pulang Pisau.

4.2 Comparison with previous fire years

A comparison of wet and dry season $PM_{2.5}$ concentrations at a remote site suggests fires increased 2023 $PM_{2.5}$ concentrations by 38.9 µg m^{-3} (33.6-54.8 µg m^{-3}), consistent with previous estimates. This reinforces that even remote locations experience substantial regional smoke forcing during severe fire years, implying broad spatial coherence in air pollution. Uda *et al.* (2019) estimated that peatland fires contributed 26 µg m^{-3} $PM_{2.5}$ to peatland fires across Central Kalimantan during the 2011-2015 period, with spatial variability ranging from 4-103 µg m^{-3}. Although Grosvenor *et al.* (2024) did not explicitly quantify the contributions of fires to $PM_{2.5}$ concentrations, they provided city wide measurements of both dry season (August-October) (97 µg m^{-3}) and background non-fire season measured $PM_{2.5}$ concentrations (14 µg m^{-3}).

The 2023 Palangka Raya dry season mean $PM_{2.5}$ concentration was 60 µg m^{-3} and the wet season mean was 13 µg m^{-3}, suggestive that the 2019 dry season fires were more severe. The comparison with 2019 also places 2023 within a continuum of severe fire years, rather than treating events as isolated episodes, strengthening interpretation of ENSO-linked variability across extremes. This is further supported when the diurnal $PM_{2.5}$ concentrations during the 2019 and 2023 dry seasons are compared. Although both dry seasons exhibit a clear dual peak in $PM_{2.5}$ concentrations 06:00 and 17:00, $PM_{2.5}$ concentrations are substantially higher in 2019, peaking at ~140 µg m^{-3} in contrast to ~60 µg m^{-3} in 2023. GFAS dry season Pulang Pisau peatland $PM_{2.5}$ fire emissions were 129.2 Gg in 2023, compared to 502.7 Gg in 2019.

4.3 Air quality exposure and guideline exceedances

In 2023, urban and rural sites exceeded the WHO guideline on 99% and 97% of days and the Indonesian guideline on 36% and 42% of days, and the remote site exceeded the guidelines on 85% (WHO) and 24% (Indonesian) of days. As conditions shifted to neutral and La Niña in the 2024 and 2025 dry seasons, higher rainfall and shallower water tables reduced fire activity

https://doi.org/10.5194/egusphere-2026-2746
Preprint. Discussion started: 25 June 2026

and associated $PM_{2.5}$ concentrations. Nonetheless, regional fire influence remained detectable in 2024, with 41% of urban dry-season days exceeding the WHO limit.

To put these impacts into context we compared exceedances using United States Environmental Protection Agency thresholds with Grosvenor *et al.* (2024). We compare a site in Kereng and a site in Palangka Raya with similar sites established in 2019 in Kereng and Palangka Raya (Table 1). The 2019 dry season was dominated by poor air quality, with 81% of days in Kereng and 73% of days in Palangka Raya classified as either unhealthy or very unhealthy. Additionally, hazardous air quality occurred on 5% of days in Kereng and 10% of days in Palangka Raya (Table 1). This highlights the severity of the air quality impact on the region during the 2019 fires. In contrast, in 2023 a large percentage of days fall into the moderate category at Kereng (39%) and Palangka Raya (32%). However, there is still widespread degradation of air quality with 61% of days in Kereng and 68% of days in Palangka Raya categorised as either unhealthy or very unhealthy (Table 1).

We also compare 2024 and 2025 to the 2023 and 2019 dry season AQI impacts. This comparison clearly indicates that in 2024 air quality was dominated by good and moderate conditions, indicating substantially less severe pollution across both Kereng and Palangkraya. 88% of days in Kereng and 93% of days in Kereng were classified as experiencing good or moderate air pollution (Table 1). In line with this, only a very small percentage of days (2% in Kereng and 6% in Palangka Raya) were classified as unhealthy or very unhealthy. In contrast, 2025 was characterised by the cleanest conditions with 100% of days categorised as good or moderate in Palangka Raya (Table 1).

Table 1. Percentage of days (%) classified by the United States Environmental Protection Agency Air Quality Index (AQI) thresholds at Kereng (KR) and Palangka Raya (PLK) during the dry seasons of 2019 (Grosvenor et al., 2024) and 2023-2025. The AQI thresholds include Good (0 – 9 μg m^{-3}), Moderate (9.1 – 35.4 μg m^{-3}), Unhealthy (Sensitive Groups) (35.5 – 55.4 μg m^{-3}), Unhealthy (55.5 –125.4 μg m^{-3}), Very Unhealthy (125.5 – 250.4 μg m^{-3}), Hazardous (level 1) (250.5 – 350.4 μg m^{-3}), Hazardous (level 2) (350.5 – 500.4 μg m^{-3}), and Extreme (>500.5 μg m^{-3}). The total number of days included in each dry season is also indicated.

Year	Good		Moderate		Unhealthy (sensitive groups)		Unhealthy		Very unhealthy		Hazardous 1		Hazardous 2		Extreme		Total Days Assessed	
	KR	PLK	KR	PLK	KR	PLK	KR	PLK	KR	PLK	KR	PLK	KR	PLK	KR	PLK	KR	PLK
2019	1	3	16	14	23	12	38	35	20	26	2	8	3	2	0	2	68	66
2023	0	0	39	32	25	29	17	17	19	22	0	0	0	0	0	0	77	77
2024	31	18	57	75	1	5	1	1	0	0	0	0	0	0	0	0	77	76
2025		36		64		0		0		0		0		0		0	-	55

https://doi.org/10.5194/egusphere-2026-2746
Preprint. Discussion started: 25 June 2026

4.4 Spatial variability and diurnal behaviour

During the 2023 El Niño dry season, low spatial variability and a pronounced dual-peak diurnal cycle indicated that regional fire emissions dominated over local sources. While during the remaining periods (2024 and 2025) a single evening peak dominated the diurnal cycle of $PM_{2.5}$. Grosvenor *et al.* (2024) observed the same dry season diurnal cycle in 2019. A morning peak in $PM_{2.5}$ concentrations occurred around 06:00 and an evening peak occurred around 17:00. They attributed the morning peak to the collapse of the boundary layer overnight which acts to trap pollutants close to the surface and increase $PM_{2.5}$ concentrations. Peak $PM_{2.5}$ concentrations were substantially higher in 2019, peaking at ~140 μg m^{-3} in contrast to ~60 μg m^{-3} in this study. This is likely a consequence of more severe fires in 2019. In contrast to this study, Grosvenor *et al.* (2024) found that although sites across Palangka Raya and Kereng had similar daily mean AQI (~175) during the 2019 dry season, the AQI interquartile range varied substantially (300-500) across sites in September when fire $PM_{2.5}$ emissions were highest (GFAS: 382.6 Gg).

4.5 Evaluation of hydrological conditions

SMAP-derived dry season mean Pulang Pisau peatland water table depth between 2023-2025 compares reasonably well to in-situ field measurements collected in Indonesian peatlands. Hooijer *et al*. (2012) monitored water table depth in drained forests in Riau between 2007 and 2010, finding levels were 33 cm (±16 cm) below the peat surface but increased to 70 cm in drained plantations. Wösten *et al.* (2008) used hydrological modelling to compare water table levels at undrained and drained sites across Central Kalimantan between 1993 and 2001. During dry years (e.g. 1997) water table depth fell to more than 40 cm below the peat surface across almost all areas of drained and undrained peatlands in October. The draw down of the water table was fastest and more severe in undrained locations where it reached a minimum of 120 cm below the peat surface. During wet years (e.g.1999) water table depth peaked above the surface (>0 cm) in undrained peatlands, while in undrained peatlands it remained below the surface (0 to 40 cm below the peat surface). Jaenicke *et al.* (2011) focussed on the 2004-2009 period across Central Kalimantan, comparing a deforested and forested site. Water table depth was ~10 to 50 cm below the peat surface in the forested, and 25 to 75 cm below the peat surface at the unforested site during the 2007 wet season. In contrast, during the 2006 El Niño dry season the water table level fell to more than 1.5 m below the peat surface in the forested site and 2 m below the peat surface at the unforested site. SMAP-derived WTD struggles to capture the extremely low water table values observed in in-situ field measurements, which is likely at least partly due to the spatial resolution of the product.

4.6 Implications for monitoring $PM_{2.5}$ concentrations using low-cost sensor networks

We demonstrate that dense low-cost sensor networks provide critical capability for detecting regional smoke events. Our network effectively distinguished regional fire pollution from local emissions and revealed ENSO-phase dependent shifts in dry season $PM_{2.5}$ concentrations. Spatial variability and $PM_{2.5}$ magnitude across sites is a simple, robust indicator of regional smoke influence and could serve as an early-warning tool for local authorities. This demonstrates the value of dense, low-cost sensor networks, which can capture local and regional pollution patterns that sparse reference grade monitors cannot.

https://doi.org/10.5194/egusphere-2026-2746
Preprint. Discussion started: 25 June 2026

Globally, few cities operate networks as dense as ours (Table 2). With 0.36 sensors per km^2, our network across Palangka Raya network is among the densest reported, comparable to Bhaktapur, Nepal, and exceeded only by Pavia, Italy. Most other networks are far sparser (0.02–0.11 sensors per km^2). Regardless of density, all low-cost networks we identified provide far better spatial coverage than relying on reference-grade monitoring alone. Thus, such networks have the potential to transform understanding of air-pollution variability and source contributions across cities and regions.

Table 2. Sensor Networks identified using Purple Air low-cost $PM_{2.5}$ sensors across cities worldwide. Sensor network name is given where a naming convention clearly exists for the Purple Air sensors in that location. City name and country are also provided. In addition, the estimated area covered by the Purple Air sensors is provided, with the total number of sensors and estimate sensor density (per km^2 and per 100 km^2) to allow comparison between networks.

Sensor Network Name	**Location**	**Area (km^2)**	**Number of sensors**	**Sensor Density (sensors per km^2)**	**Sensor Density (sensors per 100 km^2)**
KaliAQ	Palangka Raya, Indonesia	150	54	0.36	36.0
Unnamed	Sydney, Australia	2660	55	0.02	2.1
Unnamed	Bhaktapur, Nepal	77	29	0.38	37.7
PANACEA	Athens, Greece	404	46	0.11	11.4
PANACEA	Patras, Greece	747	16	0.02	2.1
P@P	Pavia, Italy	11	20	1.82	181.8
Geohealth	Lima, Peru	1056	33	0.03	3.1
Sensing Leeds	Leeds, UK	397	34	0.09	8.6

5. Conclusions

By comparing dry seasons across different ENSO phases, we show that fire-driven exceedances of air quality guidelines are tightly linked to ENSO-phase driven drought severity. More specifically, the results indicate a climate–hydrology–fire–air quality cascade in which ENSO-phase controls exposure risk through peatland moisture regulation.

The number of days exceeding WHO and Indonesian $PM_{2.5}$ limits was highest in the 2023 El Niño year and dropped sharply in 2024 and 2025 as fire activity declined. This demonstrates that exceedances are primarily controlled by fire intensity and peatland flammability. The apparent threshold like response in air quality guideline exceedance frequency suggests peat hydrology may be a critical leverage point for reducing smoke exposure through restoration and water management.

https://doi.org/10.5194/egusphere-2026-2746
Preprint. Discussion started: 25 June 2026

These findings demonstrate that ENSO-phase driven changes in peatland flammability strongly modulate dry season fire emissions and regional air quality impacts. This also suggests peat hydrological restoration should be considered not only as a fire mitigation strategy, but as a preventative air quality intervention, capable of reducing regional population smoke exposure by lowering peat flammability before severe fire conditions emerge.

More broadly, these findings demonstrate that ENSO-phase driven changes in peatland flammability strongly modulate dry season fire emissions and regional air quality impacts, and that fire management strategies may deliver benefits across a range of climate states, not just during extreme El Niño years.

Supplement link

Author contributions

Ailish M. Graham: Conceptualization (lead), Data curation (lead), Formal analysis (lead), Investigation (lead), Methodology (lead), Validation (lead), Visualization (lead), Writing – original draft (lead), Writing – review & editing (lead), Funding Acquisition (support)
Dominick V Spracklen: Methodology (supporting), Supervision (supporting), Writing – original draft (supporting), Writing – review & editing (supporting), Funding Acquisition (lead)
James B. McQuaid: data curation (support), Funding Acquisition (support)
Richard Rigby: Software (lead), Data curation (support)
Hanun Nurrahmawati: Methodology (support), Data curation (support)
Devina Ayona: Methodology (support), Data curation (support)
Resti Salmayenti: Data curation (support), Writing – review & editing (supporting)
Kitso Kusin: Methodology (support), Data curation (support)
Adi Jaya: Methodology (support), Data curation (support), Writing – review & editing (supporting)
Thomas E. L. Smith: Conceptualization (support), Methodology (support), Data curation (support), Writing – review & editing (supporting)
Annisa Alifindira: Methodology (support)
Shofwan Al Banna Choiruzzad: Methodology (support)
Richard Pope: Writing – review & editing (supporting)

Competing interests

The authors declare that they have no conflict of interest.

https://doi.org/10.5194/egusphere-2026-2746
Preprint. Discussion started: 25 June 2026

Acknowledgements

We would like to thank the Indonesian National Research & Innovation Agency (BRIN) for permission to conduct research in Indonesia. We would also like to thank the local communities in Central Kalimantan who made this research possible by hosting sensors in their villages, towns and cities. The author(s) utilized MS copilot to refine the phrasing of the drafted text. The final manuscript was thoroughly verified and approved by all authors, who retain sole accountability for the accuracy and integrity of the work.

Financial support

This study was funded by the UKRI Global Challenges Research Fund, Grant NE/T010401/1 and the National Centre for Earth Observation, Grant NE/R016518/1.

5. References

Barkjohn, K. K., Gantt, B., and Clements, A. L.: Development and application of a United States-wide correction for $PM_{2.5}$ data collected with the PurpleAir sensor, *Atmos. Meas. Tech*., **14,** 4617–4637, https://doi.org/10.5194/amt-14-4617-2021, 2021.

Chan, K., Schillereff, D.N., Baas, A.C., Chadwick, M.A., Main, B., Mulligan, M., O'Shea, F.T., Pearce, R., Smith, T.E., Van Soesbergen, A. and Tebbs, E.: Low-cost electronic sensors for environmental research: Pitfalls and opportunities. *Progress in Physical Geography: Earth and Environment*, **45**(3), pp.305-338. https://doi.org/10.1177/0309133320956567, 2021.

Crippa, P., Castruccio, S., Archer-Nicholls, S., Lebron, G. B., Kuwata, M., Thota, A., Sumin, S., Butt, E., Wiedinmyer, C., and Spracklen, D. V.: Population exposure to hazardous air quality due to the 2015 fires in Equatorial Asia, *Sci. Rep*., **6**, 37074, https://doi.org/10.1038/srep37074, 2016.

EPA: Quality Assurance Guidance Document 2.12: Monitoring $PM_{2.5}$ in Ambient Air Using Designated Reference or Class I Equivalent Methods, United States Environmental Protection Agency, https://www3.epa.gov/ttnamti1/files/ambient/pm25/qa/m212.pdf, 2016.

Frederickson, L. B., Sidaraviciute, R., Schmidt, J. A., Hertel, O., and Johnson, M. S.: Are dense networks of low-cost nodes really useful for monitoring air pollution? A case study in Staffordshire, *Atmos. Chem. Phys.*, **22,** 13949–13965, https://doi.org/10.5194/acp-22-13949-2022, 2022.

Graham, A. M., Spracklen, D. V., McQuaid, J. B., Smith, T. E. L., Nurrahmawati, H., Ayona, D., Mulawarman, H., Adam, C., Papargyropoulou, E., Rigby, R., and Padfield, R.: Updated smoke exposure estimate for Indonesian peatland fires using a

https://doi.org/10.5194/egusphere-2026-2746
Preprint. Discussion started: 25 June 2026

network of low-cost $PM_{2.5}$ sensors and a regional air quality model, *GeoHealth*, **8,** e2024GH001125, https://doi.org/10.1029/2024GH001125, 2024.

Grosvenor, M. J., Ardiyani, V., Wooster, M. J., et al.: Catastrophic impact of extreme 2019 Indonesian peatland fires on urban air quality and health, *Commun. Earth Environ*., **5,** 649, https://doi.org/10.1038/s43247-024-01813-w, 2024.

Hooijer, A., Page, S., Jauhiainen, J., Lee, W. A., Lu, X. X., Idris, A., and Anshari, G.: Subsidence and carbon loss in drained tropical peatlands, *Biogeosciences*, **9,** 1053–1071, https://doi.org/10.5194/bg-9-1053-2012, 2012.

Jaenicke, J., Englhart, S., and Siegert, F.: Monitoring the effect of restoration measures in Indonesian peatlands by radar satellite imagery, *J. Environ. Manage*., **92,** 630–638, https://doi.org/10.1016/j.jenvman.2010.10.018, 2011.

Kaiser, J. W., Heil, A., Andreae, M. O., Benedetti, A., Chubarova, N., Jones, L., Morcrette, J.-J., Razinger, M., Schultz, M. G., Suttie, M., and van der Werf, G. R.: Biomass burning emissions estimated with a global fire assimilation system based on observed fire radiative power, *Biogeosciences,* **9,** 527–554, https://doi.org/10.5194/bg-9-527-2012, 2012.

Kiely, L., Spracklen, D. V., Wiedinmyer, C., Conibear, L., Reddington, C. L., Archer-Nicholls, S., Lowe, D., Arnold, S. R., Knote, C., Khan, M. F., and Latif, M. T.: New estimate of particulate emissions from Indonesian peat fires in 2015, *Atmos. Chem. Phys.,* **19,** 11105–11121, https://doi.org/10.5194/acp-19-11105-2019, 2019.

Kiely, L., Spracklen, D. V., Wiedinmyer, C., Conibear, L., Reddington, C. L., Arnold, S. R., Knote, C., Khan, M. F., Latif, M. T., Syaufina, L., and Adrianto, H. A.: Air quality and health impacts of vegetation and peat fires in Equatorial Asia during 2004–2015, *Environ. Res. Lett.,* **15,** 094054, https://doi.org/10.1088/1748-9326/ab9a6c, 2020.

Malings, C., et al.: Fine particle mass monitoring with low-cost sensors: Corrections and long-term performance evaluation, *Aerosol Sci. Technol.,* **54,** 160–174, https://doi.org/10.1080/02786826.2019.1623863, 2019.

Mead, M. I., Castruccio, S., Latif, M. T., Nadzir, M. S. M., Dominick, D., Thota, A., and Crippa, P.: Impact of the 2015 wildfires on Malaysian air quality and exposure: a comparative study of observed and modelled data, *Environ. Res. Lett.,* **13,** 044023, https://doi.org/10.1088/1748-9326/aab4c1, 2018.

Mathieu-Campbell, M. E., Guo, C., Grieshop, A. P., and Richmond-Bryant, J.: Calibration of PurpleAir low-cost particulate matter sensors: model development for air quality under high relative humidity conditions, *Atmos. Meas. Tech.,* **17,** 6735–6749, https://doi.org/10.5194/amt-17-6735-2024, 2024.

https://doi.org/10.5194/egusphere-2026-2746
Preprint. Discussion started: 25 June 2026

McFarlane, C., Raheja, G., Malings, C., Appoh, E. K. E., Hughes, A. F., and Westervelt, D. M.: Application of Gaussian mixture regression for the correction of low-cost $PM_{2.5}$ monitoring data in Accra, Ghana, *ACS Earth Space Chem.*, **5,** 2268–2279, https://doi.org/10.1021/acsearthspacechem.1c00217, 2021.

Mulyasih, H., Akbar, L.A., Ramadhan, M.L., Cesnanda, A.F., Putra, R.A., Irwansyah, R. and Nugroho, Y.S.: Experimental study on peat fire suppression through water injection in laboratory scale. *Alexandria Engineering Journal*, **61**(12), pp.12525-12537. https://doi.org/10.1016/j.aej.2022.06.036, 2022.

NOAA: Cold & Warm Episodes by Season, https://www.cpc.ncep.noaa.gov/products/analysis_monitoring/ensostuff/ONI_v5.php, accessed 16 Feb 2026, 2026.

Page, S. E., Siegert, F., Rieley, J. O., Boehm, H. D. V., Jaya, A., and Limin, S.: The amount of carbon released from peat and forest fires in Indonesia during 1997, *Nature,* **420,** 61–65, https://doi.org/10.1038/nature01131, 2002.

Reddington, C. L., Conibear, L., Robinson, S., Knote, C., Arnold, S. R., and Spracklen, D. V.: Air pollution from forest and vegetation fires in Southeast Asia disproportionately impacts the poor, *GeoHealth,* **5,** e2021GH000418, https://doi.org/10.1029/2021GH000418, 2021.

Reichle, R.H., Liu, Q., Koster, R.D., Crow, W.T., De Lannoy, G.J., Kimball, J.S., Ardizzone, J.V., Bosch, D., Colliander, A., Cosh, M. and Kolassa, J.: Version 4 of the SMAP level-4 soil moisture algorithm and data product, *Journal of Advances in Modeling Earth Systems,* **11**(10), pp.3106-3130. https://doi.org/10.1029/2019MS001729, 2019.

Salmayenti, R., Baird, A.J., Holden, J. and Spracklen, D.V.: Drainage density and land cover interact to affect fire occurrence in Indonesian peatlands. *Environmental Research Letters*, **20**(5), p.054036. https://doi.org/10.1088/1748-9326/adc755, 2025.

Schroeder, W. and Giglio, L.: VIIRS 375 m and 750 m active fire detection data sets based on NASA VIIRS SIPS reprocessed data, NASA, https://lpdaac.usgs.gov/documents/132/VNP14_User_Guide_v1.3.pdf, accessed 28 Nov 2025, 2017.

Uda, S. K., Hein, L., and Atmoko, D.: Assessing the health impacts of peatland fires: a case study for Central Kalimantan, Indonesia, *Environ. Sci. Pollut. Res.,* **26,** 31315–31327, https://doi.org/10.1007/s11356-019-06264-x, 2019.

Wooster, M. J., Gaveau, D. L. A., Salim, M. A., Zhang, T., Xu, W., Green, D., Huijnen, V., Murdiyarso, D., Gunawan, D., Borchard, N., Schirrmann, M., Main, B., and Sepriando, A.: New tropical peatland gas and particulate emissions factors indicate 2015 Indonesian fires released far more particulate matter (but less methane) than current inventories imply, *Remote Sens.,* **10,** 495, https://doi.org/10.3390/rs10040495, 2018.

https://doi.org/10.5194/egusphere-2026-2746
Preprint. Discussion started: 25 June 2026

Wösten, J. H. M., Clymans, E., Page, S. E., Rieley, J. O., and Limin, S. H.: Peat–water interrelationships in a tropical peatland ecosystem in Southeast Asia, *Catena,* **73,** 212–224,